Monitoring the process mean when standards are unknown: A classic problem revisited

M.D. Diko
Department of Statistics
University of Pretoria
South Africa
dikomandla@gmail.com

S. Chakraborti[1]
Department of Information Systems, Statistics and Management Science,
University of Alabama
Tuscaloosa, AL 35487, U.S.A.
schakrab@cba.ua.edu

M.A. Graham
Department of Statistics
University of Pretoria
South Africa
marien.graham@up.ac.za

Abstract

One of the most common applications in statistical process monitoring is the use of control charts to monitor a process mean. In practice, this is often done with a Shewhart $\overline{X}$ chart along with a Shewhart R (or an S) chart. Thus two charts are typically used together, as a scheme, each using the 3-sigma limits. Moreover, the process mean and standard deviation are often unknown and need to be estimated before monitoring can begin. We show that there are three major issues with this monitoring scheme described in most textbooks. The first issue is not accounting for the effects of parameter estimation, which is known to degrade chart performance. The second issue is the implicit assumption that the charting statistics are both normally distributed and, accordingly, using the 3-sigma limits. The third issue is multiple testing, since two charts are used, in this scheme, at the same time. We illustrate the deleterious effects of these issues on the in-control properties of the $(\overline{X}, R)$ charting scheme and present a method for finding the correct charting constants taking proper account of these issues. Tables of the new charting constants are provided for some commonly used nominal in-control average run-length ($ICARL_0$) values and different sample sizes. This will aid in implementing the $(\overline{X}, R)$ charting scheme correctly in practice. Examples are given along with a summary and some conclusions.

Keywords: False alarm rate; Monitoring mean and variance; Multiple testing; Parameter estimation, 3-sigma limits; Shewhart $\overline{X}$ chart, Shewhart R chart

1. Introduction

For decades control charts have been used as effective tools for detecting process changes that may affect the quality of products and services. In most cases the process is assumed to be normally distributed, and the goal is to monitor the mean (μ) of the process with a Shewhart $\overline{X}$ chart. However, even though the mean μ may be the

[1] Part of the work done in the Department of Statistics, University of Pretoria, South Africa

quantity of interest, the standard deviation σ is also monitored with a Shewhart *R* (or an *S*) chart. This is because the $\overline{X}$ control chart limits depend on σ and therefore unless σ is in-control (IC), the $\overline{X}$ chart does not convey much meaning. The bottom line is that two charts are used, as a charting scheme, to make a decision about the status of the process. The process is considered to be IC whenever both charts plot within their respective control limits and display random patterns. On the other hand, the process is declared out-of-control (OOC) when at least one of the charts shows an OOC situation, such as a point outside of the control limits or points exhibiting a non-random pattern.

For simplicity we assume that the Shewhart $\overline{X}$ chart and the Shewhart *R* chart are used to monitor the process mean (μ) and the process standard deviation (σ), respectively. We use the Shewhart *R* chart even though recent literature recommends using a different spread chart, such as the Shewhart *S* chart, see for instance Mahmoud[1]. We do this because the Shewhart *R* chart is simple and continues to be used in industry. However, our ideas can easily be extended to other two-chart schemes for the mean and the variance of a normal process, including the Shewhart $(\overline{X}, S)$ charting scheme, and other more sophisticated two-chart monitoring schemes involving the cumulative sum (CUSUM) and the exponentially weighted moving average (EWMA) charts. Note that, from this point forward we will refer to the Shewhart $\overline{X}$ chart, the Shewhart *R* chart and the Shewhart *S* chart; as the $\overline{X}$ chart, the *R* chart and the *S* chart, respectively.

Even though a lot of work has been done on monitoring the mean and the standard deviation of a normally distributed process using Shewhart or Shewhart-type charts (Quesenberry[2], Chen[3,4], Chakraborti[5,6]), few studies (for example, Diko et al.

(2014)) seem to have considered the design and performance of the $\overline{X}$ and R charts as they are applied together as a charting scheme. According to the current practice, the $\overline{X}$ chart and the R chart are constructed independently, each using the estimated 3-sigma limits, which are calculated from a Phase I reference sample. We show that this practice is incorrect, which results in the average run-length (*ARL*) being significantly off from the nominal value. In fact, the *ARL* is often shorter, which implies that the false alarm rate is more than what is nominally expected. We then derive and present the new charting constants to help practitioners to run the $(\overline{X}, R)$ charting scheme at the desired nominal level.

This paper is organised as follows: we first illustrate the ideas with an example (Example 1), showing how monitoring the process mean is presently done in industry. This sets the stage. We then consider two cases (i) the case when the mean is known or specified but the standard deviation is unknown (denoted Case KU) (ii) the case when both the mean and standard deviation are unknown (denoted Case UU). The Case KU is important since it often arises in practice in meeting specifications for a process. The Case UU is the general case where not much is known about the process parameters, such as in a start-up situation. For each case, we analytically derive the unconditional in-control average run-length (denoted by *ICARL*, see Appendix A) of the $(\overline{X}, R)$ charting scheme, with the estimated 3-sigma limits. This is the IC average run-length averaged over the distribution(s) of the parameter estimator(s). We show that the values of the *ICARL* can be far lower than the specified nominal IC average run-length, denoted by $ICARL_0$. This is obviously a major issue since there will be lots of unexpected false alarms. Following this, we present a method for correcting these control limits; which accounts for the effects of parameter estimation, use of the estimated 3-sigma limits and multiple testing. Finally, we give an illustration using the same data from the first example but applying the corrected limits and contrast the results. It is seen that the corrected limits can alter decisions. We conclude with a summary and recommendations.

1.1. Example 1

To set the stage, we constructed the $\overline{X}$ chart and the R chart, with the estimated 3-sigma limits, in Case UU, using the data set on measurements of the flow width of the Hard-Bake process (see Montgomery[7] (p. 244)). This data set contains m = 20 Phase I subgroups, each of size n = 5. The average of the Phase I sample means and ranges are $\overline{\overline{X}} = 1.5056$ and $\overline{R} = 0.3252$, respectively. The resulting $\overline{X}$ and R charts, with the estimated 3-sigma limits, are shown in Figures 1a and b, respectively.

Figures 1a and b help to illustrate the $(\overline{X}, R)$ charting scheme, with the estimated 3-sigma limits, as presently used in the industry. As always, the R chart is examined first. This is done because the control limits of the $\overline{X}$ chart depend on the estimate of process variability (see Equations (1) and (4)). From Figure 1b it is seen that the variability is IC, and so we go on to examine the $\overline{X}$ chart in Figure 1a. Figure 1a shows that the process mean is IC until the 18$^{\text{th}}$ sample when the $\overline{X}$ chart gives a signal. However, whether this is a genuine signal or a false alarm could be questioned based on three issues.

The first issue is the effect of parameter estimation, which is not accounted for by the control limits used in either of these charts. It is well-known that using parameter estimates instead of known parameters without accounting for the additional variability introduced by parameter estimation degrades chart performance (see Jensen et al.[8], Quesenberry[2]). In fact, based on the current available information in the literature, we suspect that the unconditional *ICARL* for the charting scheme

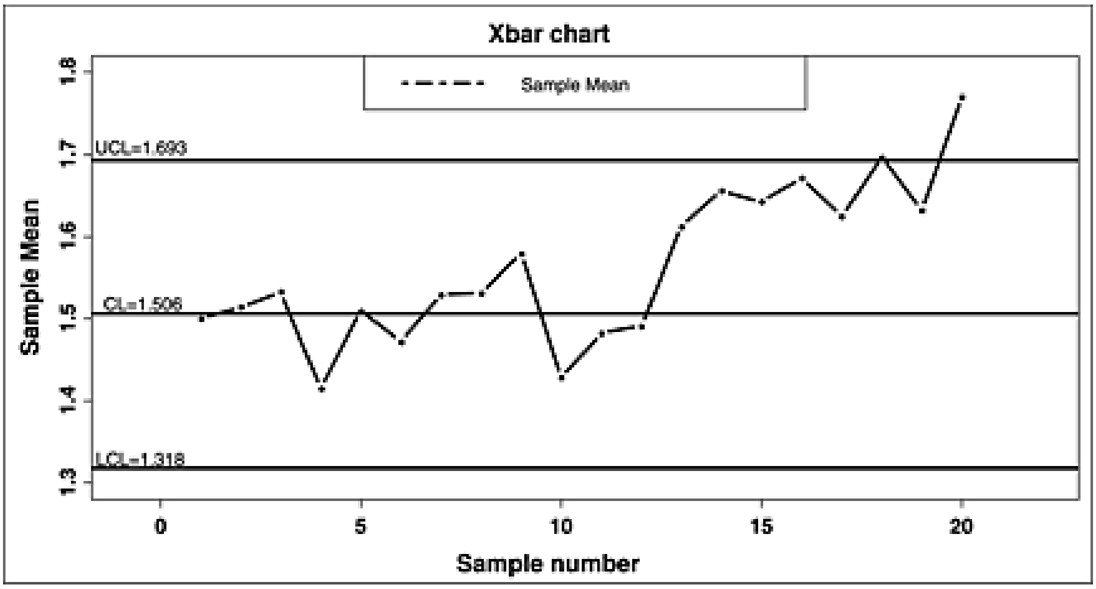

a

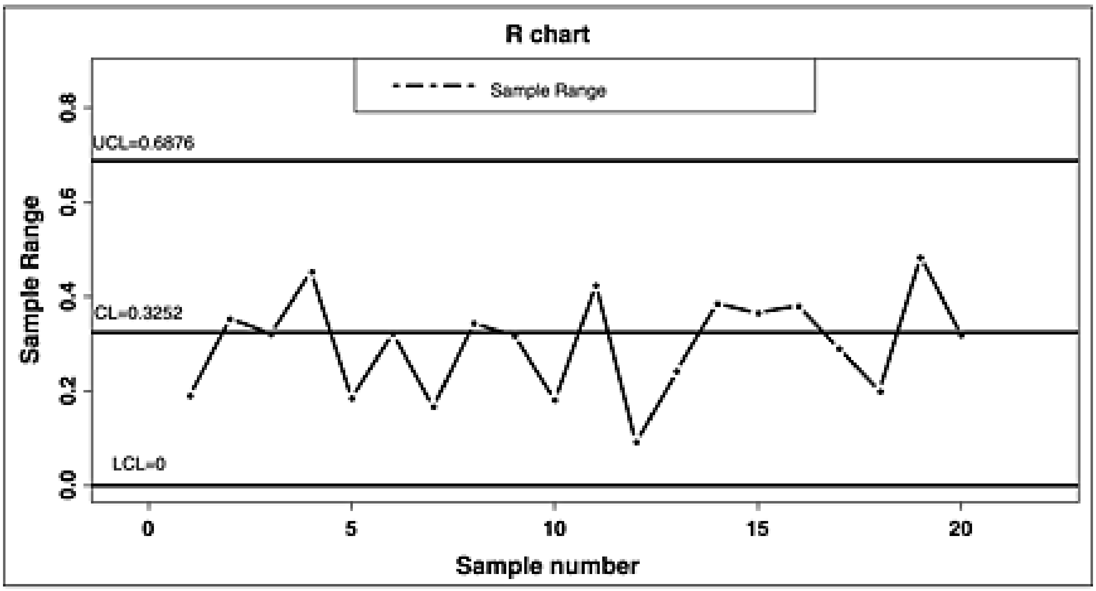

b

Figure 1. **(**a) The $\overline{X}$ chart for the mean, with the estimated 3-sigma limits, for the data from Montgomery[8] (p. 244). (b) The *R* chart for variability, with the estimated 3-sigma limits, for the data from Montgomery[8] (p. 244). LCL, lower control limit; CL, center line; UCL, upper control limit

would be less than the nominal $ICARL_0$, so that the false alarms rate (*FAR*) is increased.

The second issue relates to the standard practice of using the estimated 3-sigma control limits in the two component charts. This is a common practice and is recommended in most textbooks, including Montgomery[7]. However, the plotting statistics, $\overline{X}$ and *R*, each has a different sampling distribution, and thus each component chart, each with the estimated 3-sigma limits, has a different unconditional *ICARL*, which can be different from the nominal $ICARL_0$. This, in fact, is shown to be true, which in turn yields a completely different unconditional *ICARL* for the two-chart $(\overline{X}, R)$ scheme.

The third issue relates to the issue of multiple testing. As two charts are used simultaneously in the decision making process, unless proper adjustments are made, the charting scheme does not deliver the nominal $ICARL_0$. In fact, as will be seen in Tables 1 and 3, that the unconditional *ICARL* of the charting scheme is far lower than the nominal $ICARL_0$. This means that many more false alarms are issued, leading to faulty decisions, possible work stoppages and reducing the value of the charting scheme. Note that the fact that the two component charting statistics, $\overline{X}$ and R, are independent under normality does not solve the problem induced by multiple testing; however it does play a role in finding a correction.

In summary, while monitoring the mean, when parameters are estimated, the control limits of the $(\overline{X}, R)$ charting scheme need to be corrected so that the effects of parameter estimation are correctly accounted for along with the effects of using the estimated 3-sigma limits and multiple testing. We do this by first using the conditioning technique developed in Chakraborti[5], then applying a correction to take account of multiple testing and finally using the probability limits. We start with Case KU.

2. Mean known and standard deviation unknown (Case KU)

In a number of practical situations, one has a specified value of the mean of the process to monitor, but the standard deviation of the process is unknown. This is Case KU. We now consider the $(\overline{X}, R)$ charting scheme, with the estimated 3-sigma limits, in this case. We show analytically that the unconditional *ICARL* values of this scheme differ dramatically from the nominal $ICARL_0$. We then use this result to calculate the correct charting constants that deliver the nominal $ICARL_0$. However, since the unconditional *ICARL* of the $(\overline{X}, R)$ charting scheme depends on the unconditional *ICARL* of its two component charts, we review the two component charts first. We start with the $\overline{X}$ chart with the estimated 3-sigma limits.

2.1. Shewhart $\overline{X}$ chart, with the estimated 3-sigma limits

When any of the process parameters are unknown, they are estimated from a Phase I reference data. Let X_{ij}, i=1,2,…,m and j=1,2,…,n denote the IC Phase I data from a normal distribution with a specified mean μ_0 and an unknown standard deviation σ, where *m* is the number of Phase I subgroups and *n* is the subgroup size. The plotting statistic for the $\overline{X}$ chart, with the estimated 3-sigma limits, in Phase II, is the sample mean $\overline{X}_i$, $i = m+1, m+2, \ldots$. It is well-known that the IC distribution of the sample mean is normal with mean μ_0 and variance σ^2/n.

Typically, the estimated lower and upper control limits of the $\overline{X}$ chart, with the estimated 3-sigma limits, are expressed as

$$L\hat{C}L_{xbar} = \mu_0 - 3\frac{\hat{\sigma}}{\sqrt{n}}$$
$$U\hat{C}L_{xbar} = \mu_0 + 3\frac{\hat{\sigma}}{\sqrt{n}} \quad (1)$$

respectively, where $\hat{\sigma} = \frac{\overline{R}}{d_2}$ is the unbiased estimator of σ, $\overline{R}$ is the average of the Phase I sample ranges and d_2 is the unbiasing constant, defined later.

Note that, the performance of a Phase II control chart is judged in terms of its run-length distribution and certain characteristics, such as the *ARL* and the standard deviation of the run-length (denoted by *SDRL*). The run-length (denoted by *N*) is a discrete random variable that represents the number of subgroups which must be collected in order for the chart to give the first signal. It is well-known that when the mean and the variance of a process are both known or specified (the so-called standards known case, denoted by Case KK), and the process is IC, the run-length distribution is geometric with the parameter equal to the nominal false alarm rate (denoted by FAR_0) and mean equal to the nominal $ICARL_0$. However, this is not the case when any of the parameters is unknown and are estimated. Thus, assuming that the process is IC and that some value(s) of the Phase I parameter estimator(s) have been observed, it is now well known (see, e.g., Chakraborti[5]) that *N* follows a geometric distribution with the parameter equal to the conditional false alarm rate (denoted by *CFAR*) and mean equal to the conditional in-control average run-length (denoted by *CICARL*). The word conditional refers to the fact that these values are calculated for given values of the parameter estimates, for the given Phase I sample. Thus, the *CFAR* and *CICARL* are random variables and so their values can be radically different from the nominal FAR_0 and the nominal $ICARL_0$, respectively. Studies of control chart performance have mostly focused on the unconditional run-length distribution and its associated characteristics, such as the unconditional *ICARL* (see Jensen et al.[8]). Accordingly, in this paper, we use the unconditional *ICARL* to evaluate chart performance and to make design recommendations when any of the process parameters are unknown.

Against this background, we derive an expression for the unconditional *ICARL* for the $\overline{X}$ chart, with the estimated 3-sigma limits, in Case KU (see (A4) and (A3) in Appendix A) and tabulate it in Panel (a) of Table 1 for n = 5 and for various values of m. The percentage difference, PD = $100\left(\frac{\text{attained unconditional } ICARL - 370}{370}\right)$, is also shown for each m.

Table 1. The attained unconditional *ICARL* values and the percentage difference for the $(\overline{X}, R)$ charting scheme and its component charts, with the estimated 3-sigma limits, in Case KU, for various values of m and n = 5 and the nominal $ICARL_0$ = 370

m	**(a) $\overline{X}$ chart**		**(b) R chart**		**(c) $(\overline{X}, R)$ charting scheme**	
	ICARL	**PD**	***ICARL***	**PD**	***ICARL***	**PD**
5	3169	756%	10587	2758%	2228	502%
10	884	139%	1000	170%	445	20%
20	550	49%	422	14%	235	-37%
30	479	29%	332	-10%	194	-48%
50	430	16%	278	-25%	168	-55%
100	399	8%	245	-34%	152	-59%
500	375	2%	222	-40%	140	-62%
$\boldsymbol{ICARL_0}$	**370**		**370**		**370**	

An examination of Panel (a) in Table 1 reveals some interesting facts. For all values of m, the PD values differ from zero, with PD > (<) 0 indicating that the attained unconditional *ICARL* value is greater (smaller) than the nominal $ICARL_0$ = 370. It can be seen that the attained unconditional *ICRL* values differ (sometimes dramatically) from the nominal $ICARL_0$ = 370, as the absolute values of the PD range from as little as 2% (m = 500) to as much as 756% (m = 5). Although, in general, a small positive difference (< 10%) between the attained and the nominal values may be acceptable but not for the magnitudes that are seen. For example, for m = 30, which is often recommended in textbooks, the attained unconditional *ICARL* value for the scheme is 49% above the nominal value, which is unacceptable. However, the attained unconditional *ICARL* values converge to the nominal $ICARL_0$ = 370 value of 370 as m increases, which is to be expected for the $\overline{X}$ chart. But, this convergence is not seen for the R chart as well as for the two-chart $(\overline{X}, R)$ charting scheme. We discuss these next. We start with the R chart.

2.2. Shewhart *R* control chart, with the estimated 3-sigma limits

The plotting statistic for the R chart, with the estimated 3-sigma limits, is the sample range R_i. For a nominal $ICARL_0 = 370$, the lower and upper control limits of this chart are given in Montgomery[7], Chapter 6, as

$$\begin{aligned} L\hat{C}L_R &= \left(1 - \frac{3d_3}{d_2}\right)\overline{R} = D_3\overline{R} \\ U\hat{C}L_R &= \left(1 + \frac{3d_3}{d_2}\right)\overline{R} = D_4\overline{R} \end{aligned} \quad (2)$$

respectively, where $d_2 = E(W)$ and $d_3 = \sqrt{Var(W)}$ are the mean and the standard deviation of the IC distribution of the sample relative range $W_i = \frac{R_i}{\sigma}$, respectively.

The expression for the unconditional *ICARL* of the R chart, with the estimated

3-sigma limits, in Case KU, is derived in Appendix A (see (A8) and (A7)) and is tabulated in Panel (b) of Table 1 for n = 5 and various values of m. The message is really bad. For all values of m, it can be seen that the attained unconditional *ICARL* values differ (sometimes dramatically) from the nominal $ICARL_0$ = 370, since the absolute value of the PD ranges from as little as 10% (m = 30) to as much as 2758% (m = 5). Therefore, in Case KU, the R chart, with the estimated 3-sigma limits, has the unconditional *ICARL* values that are not only very different from the nominal $ICARL_0$ = 370, but are also very different from the unconditional *ICARL* values of the $\overline{X}$ chart with the estimated 3-sigma limits. Furthermore, even more striking is the fact that, unlike the $\overline{X}$ chart, the attained unconditional *ICARL* values for the R chart do not converge to the $ICARL_0$ = 370 as m increases. This is alarming, and can be attributed to the failure of the normal approximation (instead of the exact sampling distribution of R_i) along with the use of the estimated 3-sigma limits to construct the classical R chart.

In summary, using the normal approximation along with the 3-sigma limits to construct the R chart is highly aggravated by the effects of parameter estimation, so much so that even if the Phase I sample size is increased dramatically, it does not guarantee the desired nominal performance and, in fact, it becomes counterproductive.

Next we discuss the effects of multiple testing, that is, the use of the $\overline{X}$ and R charts, with the estimated 3-sigma limits, in order to monitor the mean of the process.

2.3. Shewhart $(\overline{X}, R)$ charting scheme, with the estimated 3-sigma limits

As noted before, in practice, the $\overline{X}$ chart with the estimated 3-sigma limits is used together with a spread chart, such as the *R* chart, with the estimated 3-sigma limits, to make decisions about the status (IC or OOC) of a process. This charting scheme gives a signal when at least one of the two component charts, the $\overline{X}$ or the *R* chart, signals. It will be seen that the unconditional *ICARL* for the two-chart $(\overline{X}, R)$ scheme is far different from the nominal $ICARL_0 = 370$, and is completely different to the unconditional *ICARL* of its two component charts.

The unconditional *ICARL* of the $(\overline{X}, R)$ charting scheme, with the estimated 3-sigma limits, in Case KU, is derived in Appendix A (see (A12) and (A11)) and is tabulated in Panel I of Table 1 for *n* = 5 and various values of *m*. From Table 1 it can be seen that the unconditional *ICARL* values in Panel I are less than the corresponding unconditional *ICARL* values for the component charts in Panels (a) and (b), respectively. This implies that the $(\overline{X}, R)$ charting scheme, with the estimated 3-sigma limits, issues false alarms, on an average, quicker than its component charts. Furthermore, for *m* = 5 we have PD = 502%, this suggests that the unconditional *ICARL* values for the $(\overline{X}, R)$ charting scheme can be approximately 6 times more than the nominal $ICARL_0$ = 370. For *m* around 20-30, which is often recommended in textbooks, the attained unconditional *ICARL* values for the scheme are 37% to 48% below the nominal value, which indicates many more false alarms than expected. Interestingly, for *m* = 50, 100, 500 the attained unconditional *ICARL* values for the scheme range between 55% and 62% below the nominal value. This is counter intuitive, because increasing the Phase I sample size is expected to decrease the false alarm rate and not to increase it. Clearly, the $(\overline{X}, R)$ charting scheme, with the estimated 3-sigma limits, in Case KU, does not perform as nominally expected. Thus, the control limits of the component charts need to be adjusted such that the two-chart $(\overline{X}, R)$ scheme delivers the nominal $ICARL_0 = 370$. This is described next.

2.4. New control limits corrected for parameter estimation, the estimated 3-sigma limits and multiplicity effects

We understand the need to select the control limits on the component charts of the $(\overline{X}, R)$ charting scheme in a way that accounts for the additional variability caused by parameter estimation, corrects for the use of the estimated 3-sigma limits (implicit normal approximation for both charting statistics) along with the multiple testing issue, as a function of the available data. We accomplish this by first using the conditioning technique developed in Chakraborti[5], then applying the correction (due to multiple testing) and finally using probability limits. This is described next.

The unconditional *ICARL* of the $(\overline{X}, R)$ charting scheme, with the estimated probability limits, in Case KU, can be expressed as (see (A14) in Appendix A)

$$ICARL_{two-chart}(m,n,p) = \int_0^\infty \left[CFAR_{two-chart}(u,m,n,p)\right]^{-1} g(u)du$$

where $CFAR_{two-chart}(u,m,n,p)$ denotes the conditional false alarm rate (see (A13) in Appendix A) of the $(\overline{X}, R)$ charting scheme, with the estimated probability limits, and $g(u)$ is the density function of a random variable U, following a chi-square distribution with v degrees of freedom. Note that, by averaging the $\left[CFAR_{two-chart}(u,m,n,p)\right]^{-1}$ over the distribution of U, the effects of parameter estimation are accounted for. Further, by using the probability limits and the joint distribution of $\overline{X}_i$ and R_i, to calculate $CFAR_{two-chart}(u,m,n,p)$ in (A13) of Appendix A, the issues of estimated 3-sigma limits and multiplicity are also accounted for, respectively. Thus, for some given value of $ICARL_0$, *m* and *n*, we solve the following equation

$$\int_0^\infty \left[CFAR_{two-chart}(u,m,n,p)\right]^{-1} g(u)du = ICARL_0 \tag{3}$$

for *p*, using the software package R. Once p is found, the corrected (probability) control limits for the $\overline{X}$ and the *R* charts are found from the corresponding percentiles of the standard normal distribution and the distribution of the relative range, respectively. Some results are shown in Table 2.

Table 2 shows the new charting constants for the $(\overline{X},R)$ charting scheme in Case KU. For the nominal $ICARL_0 = 370$, it is seen that the charting constants of the $\overline{X}$ chart range from *k* = 3.198 to *k* = 3.260. These values are approximately 7% to 9% greater than the conventional charting constant *k* = 3 in Equations (1) and (2), respectively. This means that the $\overline{X}$ chart constructed, using the corrected charting constants in Table 2, will have wider control limits. This will help in reducing the higher false alarm rate (or increasing the unconditional *ICARL*) of the overall $(\overline{X},R)$ charting scheme. In addition, for the *R* chart, note that using the probability limits along with the charting constants in Table 2 ensures that the *LCL* of the *R* chart is never negative. This means that decreases in the process standard deviation that are often undetected by the conventional *R* chart (the *LCL* is negative and hence set equal to 0) will now also be detected by the $(\overline{X},R)$ charting scheme, with corrected control limits. Further, using the R code provided in B1 of Appendix B, it can be shown that

Table 2. New charting constants for the $(\overline{X}, R)$ charting scheme in Case KU for various values of *m* and *n* and $ICARL_0$ = 370 and 500, respectively.

		(a) $ICARL_0$=370				(b) $ICARL_0$=500			
n	***m***	***p***	$\overline{X}$ **chart**	***R*** **chart**		***p***	$\overline{X}$ **chart**	***R*** **chart**	
5	**5**	0.001288	3.219	0.329	5.636	0.000956	3.303	0.305	5.737
	10	0.001357	3.204	0.333	5.618	0.001008	3.288	0.309	5.719
	20	0.001382	3.198	0.335	5.611	0.001027	3.283	0.310	5.713
	30	0.001385	3.198	0.335	5.611	0.001028	3.283	0.310	5.713
	50	0.001380	3.199	0.334	5.612	0.001024	3.284	0.310	5.714
	75	0.001375	3.200	0.334	5.614	0.001020	3.285	0.310	5.715
	100	0.001371	3.201	0.334	5.615	0.001016	3.286	0.310	5.716
	500	0.001357	3.204	0.333	5.618	0.001005	3.289	0.309	5.720
10	**5**	0.001114	3.260	1.009	6.162	0.000822	3.345	0.972	6.257
	10	0.001222	3.234	1.020	6.132	0.000903	3.319	0.983	6.228
	20	0.001288	3.219	1.027	6.116	0.000953	3.304	0.989	6.211
	30	0.001311	3.214	1.029	6.111	0.000970	3.299	0.992	6.205
	50	0.001329	3.210	1.031	6.105	0.000984	3.295	0.993	6.201
	75	0.001337	3.208	1.032	6.103	0.000990	3.293	0.994	6.199
	100	0.001342	3.207	1.032	6.102	0.000993	3.293	0.994	6.198
	500	0.001350	3.205	1.033	6.101	0.000999	3.291	0.995	6.196

the charting constants in Table 2 perform as specified, i.e. they deliver the desired nominal $ICARL_0$.

Next, we consider the $(\overline{X}, R)$ charting scheme with the estimated 3-sigma limits in Case UU. Recall that this is the situation when both the process mean and the standard deviations are unknown.

3. Mean and standard deviation both unknown (Case UU)

Again, since the properties of the charting scheme depend on the properties of its component charts, we review the component charts first. We assume that a Phase I sample of reference data, *m* subgroups, each of size *n*, is available for parameter estimation.

3.1. Shewhart $\overline{X}$ control chart, with the estimated 3-sigma limits

In Case UU, for a nominal $ICARL_0$ = 370, the $\overline{X}$ chart, with the estimated 3-sigma limits, is given in Montgomery[7], Chapter 6 by

$$\begin{aligned} LCL_{xbar} &= \overline{\overline{X}} - \frac{3}{d_2\sqrt{n}}\overline{R} = \overline{\overline{X}} - A_2\overline{R} \\ UCL_{xbar} &= \overline{\overline{X}} + \frac{3}{d_2\sqrt{n}}\overline{R} = \overline{\overline{X}} + A_2\overline{R} \end{aligned} \tag{4}$$

respectively. Next, we study the IC performance of this chart. As in Case KU, we will see that the unconditional *ICARL* of the scheme can be very different from the nominal $ICARL_0$.

The unconditional *ICARL* for the $\overline{X}$ chart, with the estimated 3-sigma limits, in Case UU, is derived in Appendix A (see (A18) and (A17)) and is tabulated in Panel (a) of Table 3 for *n* = 5 and various values of *m*. Similar to Case KU (see Table 1), the PD values are also given. It can be seen that the attained unconditional *ICARL* values differ (sometimes dramatically) from the nominal value, since the PD values range from as little as 1% (m = 500) to as much as 352% (m = 5). Note also that as in Case KU, the PD values are all positive. Also, the attained unconditional *ICARL* values converge to the nominal $ICARL_0$ = 370 as m increases. Again, this convergence is not seen for the R chart as well as for the two-chart $(\bar{X}, R)$ charting scheme. Since the R chart, with the estimated 3-sigma limits, has been discussed earlier in Case KU; we move on to discuss the $(\bar{X}, R)$ charting scheme, with the estimated 3-sigma limits, in Case UU.

Table 3. The attained unconditional *ICARL* values and the percentage difference for the $(\bar{X}, R)$ charting scheme and its component charts, with the estimated 3-sigma limits, in Case UU, for various values of m and n = 5 and the nominal $ICARL_0$ = 370

m	(a) $\bar{X}$ chart		(b) R chart		(c) $(\bar{X}, R)$ charting scheme	
	ICARL	**PD**	***ICARL***	**PD**	***ICARL***	**PD**
5	1675	352%	10587	2758%	1259	240%
10	624	69%	1000	170%	349	-6%
20	453	22%	422	14%	211	-43%
30	417	13%	332	-10%	182	-51%
50	395	7%	278	-25%	162	-56%
100	381	3%	245	-34%	149	-60%
500	372	1%	222	-40%	139	-62%
$\boldsymbol{ICARL_0}$	**370**		**370**		**370**	

3.2. The Shewhart $(\bar{X}, R)$ charting scheme, with the estimated 3-sigma limits

As noted before, in practice, the $\bar{X}$ chart, with the estimated 3-sigma limits, and a spread chart, such as the R chart, also with the estimated 3-sigma limits, are used together to make decisions about the status (IC or OOC) of a process. This charting scheme gives a signal when at least one of the two component charts, the $\overline{X}$ or the R chart, signals. We now study the IC performance of this two-chart scheme in Case UU.

The unconditional *ICARL* of the $(\overline{X}, R)$ charting scheme, with the estimated 3-sigma limits, in Case UU, is derived in Appendix A (see (A22) and (A21)) and is tabulated in Panel I of Table 3 for n = 5 and various values of m. The pattern of the results is similar to those in Case KU. Again, it can be seen that the unconditional *ICARL* values in Panel I are less than the corresponding unconditional *ICARL* values for the component charts in Panels (a) and (b), respectively. Furthermore, for m = 5, the attained unconditional *ICARL* value is 240% above the nominal value. For m around 20 to 30, which is often recommended in textbooks, the attained unconditional *ICARL* values for the scheme are 43% to 51% below the nominal value, which indicates many more false alarms than expected. For m = 50, 100, 500, the attained unconditional *ICARL* values for the scheme are 56% to 62% below the nominal value, which indicates even more false alarms than nominally expected, even though the Phase I sample has been increased. On the whole, these results show that using the $\overline{X}$ chart and the R chart, with the estimated 3-sigma limits, together in a charting scheme reduces the unconditional *ICARL* and hence increases the *FAR* by a substantial amount. This should be a cause for great concern. Again, as we did for Case KU, we need to adjust the control limits on the component charts in a way that accounts for parameter estimation, using the estimated 3-sigma limits and multiple testing; otherwise the charting scheme runs the risk of being too expensive and hence useless in practice. This is described next.

3.3. New control limits corrected for parameter estimation, 3-sigma limits and multiplicity effects, in Case UU

The method for finding the new charting constants for the $(\overline{X}, R)$ charting scheme, in Case UU, is similar to the method that was described for Case KU. First we derive an analytical expression for the unconditional *ICARL* (see (A23) and A(24) in Appendix A) and then for a given $ICARL_0$, *m* and *n*, we solve the following equation

$$\int_0^{\infty}\int_{-\infty}^{\infty}\left[CFAR_{two-chart}(z,u,m,n,p)\right]^{-1}\phi(z)g(u)dzdu = ICARL_0 \qquad (5)$$

for *p*, where ϕ is the density function of the standard normal variable. Once p is found, the correct probability control limits for the $\overline{X}$ and *R* charts are found from the corresponding percentiles of the standard normal distribution and the distribution of the relative range, respectively. The software package R is used to solve equation (5). Some results are shown in Table 4.

Using the R code in B2 of Appendix B, it can be verified that the charting constants in Table 4 yield the unconditional *ICARL* values that are equal to the nominal $ICARL_0$ values 370 and 500. Next, we illustrate how Table 4 can be used to implement the $(\overline{X}, R)$ charting scheme, with the corrected limits, in Case UU. We then compare the corrected limits against the estimated 3-sigma limits in Example 1. Keep in mind that the estimated 3-sigma control limits in Example 1 have not been corrected for parameter estimation, normal approximation and multiple testing.

Table 4. New charting constants for the $(\overline{X}, R)$ charting scheme in Case UU for various values of *m* and *n* with $ICARL_0$ = 370 and 500, respectively

		(a) $ICARL_0$=370				(b) $ICARL_0$=500			
n	***m***	***p***	**$\overline{X}$ chart**	***R* chart**		***p***	**$\overline{X}$ chart**	***R* chart**	
5	**5**	0.001025	3.284	0.310	5.713	0.000758	3.368	0.287	5.814
	10	0.001164	3.248	0.320	5.670	0.000862	3.332	0.297	5.772
	20	0.001256	3.226	0.327	5.645	0.000929	3.311	0.303	5.747
	30	0.001290	3.218	0.329	5.636	0.000955	3.303	0.305	5.737
	50	0.001318	3.212	0.331	5.628	0.000975	3.298	0.306	5.73
	75	0.001331	3.209	0.331	5.625	0.000985	3.295	0.307	5.727
	100	0.001337	3.208	0.332	5.623	0.00099	3.293	0.307	5.725
10	**5**	0.000855	3.334	0.976	6.245	0.000627	3.420	0.940	6.341
	10	0.00103	3.282	0.999	6.186	0.000758	3.368	0.962	6.282
	20	0.001163	3.248	1.014	6.148	0.000857	3.334	0.977	6.244
	30	0.001217	3.235	1.020	6.134	0.000899	3.320	0.982	6.229
	50	0.001267	3.223	1.025	6.121	0.000936	3.309	0.987	6.217
	75	0.001294	3.217	1.027	6.114	0.000957	3.303	0.990	6.210
	100	0.001308	3.214	1.029	6.111	0.000967	3.300	0.991	6.206

3.4 Example 2

Again, we use the data set used in Example 1, from Montgomery[7] (p. 244), on the measurements of the flow width of a Hard-Bake process. Recall that, for this data set, both the mean and standard deviation are unknown (Case UU). Using Table 4 and the Phase I estimates of the process mean and standard deviation given in Example 1, the corrected control limits for the charting scheme are calculated as follows

$$U\hat{C}L_{xbar} = \bar{\bar{X}} + 3.284 \times \frac{\bar{R}}{d_2\sqrt{n}} = 1.5056 + 3.226 \times \frac{0.3252}{2.326 \times \sqrt{5}} = 1.7073$$

$$L\hat{C}L_{xbar} = \bar{\bar{X}} - 3.284 \frac{\bar{R}}{d_2\sqrt{n}} = 1.5056 - 3.226 \times \frac{0.3252}{2.326 \times \sqrt{5}} = 1.3039$$

$$U\hat{C}L_R = F_W^{-1}(1 - D/2)\frac{\bar{R}}{d_2} = 5.645 \times \frac{0.3252}{2.326} = 0.7892$$

$$L\hat{C}L_R = F_W^{-1}(D/2)\frac{\bar{R}}{d_2} = 0.327 \times \frac{0.3252}{2.326} = 0.0457.$$

Note that for m = 20, n = 5 and $ICARL_0$ = 370, the charting constant for the $\bar{X}$ chart is k = 3.226 from Table 4. This value is 7.5% larger than the conventional Shewhart charting constant k = 3. Note also that, unlike the $L\hat{C}L_R$ of the R chart, with the estimated 3-sigma limits (see Example 1) the $L\hat{C}L_R$ here (with the corrected limits) is no longer equal to zero but is equal to 0.0457, hence the R chart with corrected limits can detect decreases in the process standard deviation.

Figures 4a and b help to compare the corrected limits and the 3-sigma limits for the data in Montgomery[7] (p. 244).

From Figures 2a and 2b it can be seen that the corrected limits, for both charts, are slightly wider than the estimated 3-sigma limits. The 18th point on the $\bar{X}$ chart now plots IC and thus, what we initially thought to be a signal at the 18th sample on the $\bar{X}$ chart, in Example 1, now turns out to be a false alarm. This illustrates the possible price currently paid by the practitioners while using the classical limits to construct the $\bar{X}$ and R charts. Both the corrected and the uncorrected charts signal on the 20th sample, indicating a shift in the process mean.

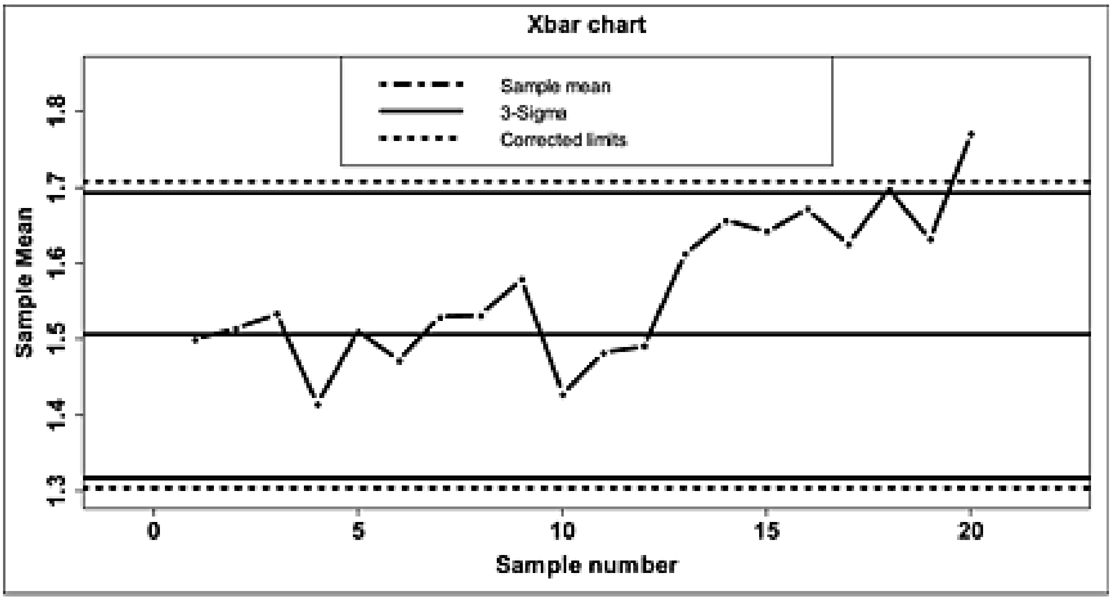

a

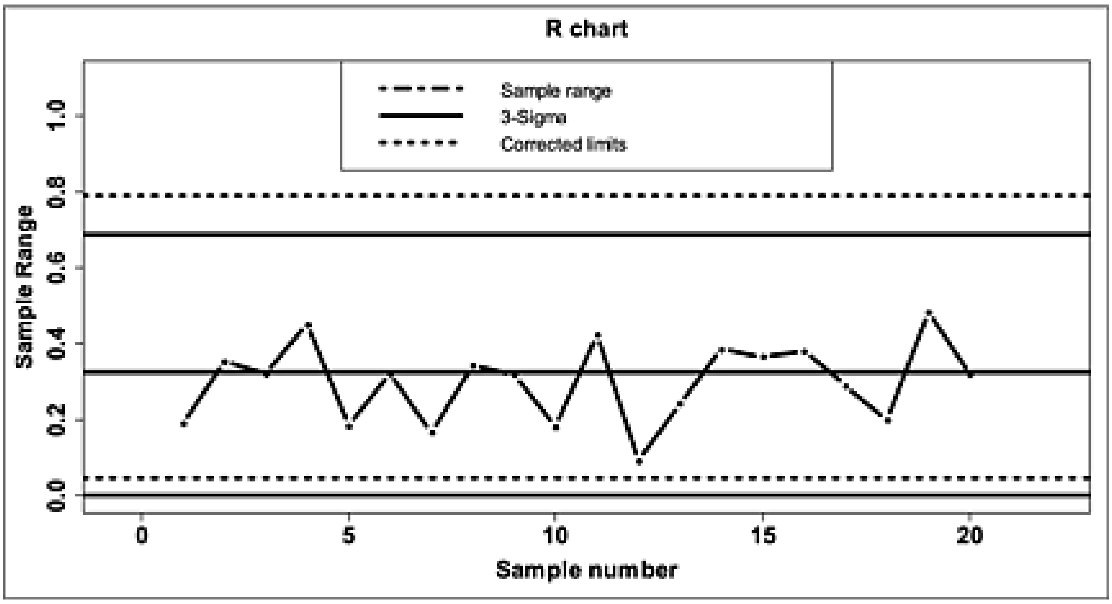

b

Figure 2. (a) The $\overline{X}$ chart for the mean with the corrected and the estimated 3-sigma (uncorrected) limits and (b) The *R* chart for variability with the corrected limits and the estimated 3-sigma (uncorrected) limits for the data from Montgomery[8] (p. 244)

Thus, using the corrected charting constants in Table 4 is recommended, because it keeps the unconditional *ICARL* at the desired nominal level.

4. Summary and Conclusion

When monitoring a process mean with a $\overline{X}$ chart, the process standard deviation is monitored first with a spread chart, such as the R chart. However, although these charts are used together, as a $(\overline{X}, R)$ charting scheme, they are often constructed individually using the estimated 3-sigma limits (see e.g., Montgomery[7]). When parameters (standards) are unknown, they are estimated from a Phase I analysis of retrospective data. We show that in the mean known and variance unknown case (Case KU) and in the mean and variance both unknown case (Case UU), the $(\overline{X}, R)$ charting scheme with estimated 3-sigma limits does not perform as expected due to (i) unaccounted parameter estimation (ii) using the incorrect assumption that the charting statistics are normally distributed and thus using the estimated 3-sigma limits for each chart and (iii) unaccounted multiple testing (or multiplicity). As a result, the false alarm rate can be very different from what is nominal, sometimes almost tripled, which obviously leads to faulty decisions, possible work stoppages and reducing the value of the charting scheme. A method for correcting the limits, taking proper account of these issues is presented in this paper. Along with the necessary theoretical derivations, a table of the new charting constants is provided for each of Case KU and Case UU, respectively. Our new charting constants help run the control charting scheme at the desired (nominal) $ICARL_0$ level. We encourage practitioners to use our tables of new charting constants to implement the $(\overline{X}, R)$ charting scheme in practice. Our ideas can be extended to other two-chart monitoring schemes, including the CUSUM and EWMA for the mean and the variance of a normal process.

Acknowledgements

Part of this work was supported by the SARCHI Chair at the University of Pretoria. Marien Graham's research was supported in part by the National Research Foundation (Thuthuka programme: TTK20100724000013247, Grant number: 76219).

References

1. Mahmoud, M.A., Henderson, G.R., Epprecht, E.K. and Woodall, W.H. (2010). "Estimating the standard deviation in quality-control applications." *Journal of Quality Technology*, 42 (4): 348-357.

2. Quesenberry, C.P. (1993). "The effect of sample size on estimated limits for the $\overline{X}$ and X control charts." *Journal of Quality Technology*, 25 (4), 237–247.

3. Chen, G. (1997). "The mean and standard deviation of the run-length distribution of $\overline{X}$ charts when control limits are estimated." *Statistica Sinica*, 7 (3): 789-798.

4. Chen, G. (1998). "The run length distributions of the R, s and s^2 control charts when σ is estimated." *The Canadian Journal of Statistics*, 26 (2): 311-322.

5. Chakraborti, S. (2000). "Run length, average run length and false alarm rate of Shewhart $\overline{X}$ chart: exact derivations by conditioning." *Communications in Statistics: Simulation and Computation*, 29 (1): 61-81.

6. Chakraborti, S. (2006). "Parameter estimation and design considerations in prospective applications of the $\overline{X}$ chart." *Journal of Applied Statistics*, 33 (4): 439-459.

7. Montgomery, D.C. (2013). Statistical Quality Control: A Modern Introduction, 7th ed., John Wiley & Sons, Singapore Pty. Ltd.

8. Jensen, W.A., Jones-Farmer, L.A., Champ, C.W. and Woodall, W.H. (2006). "Effects of parameter estimation on control chart properties: A literature review." *Journal of Quality Technology*, 38 (4), 349-364.

9. Champ, C.W., Jones, L.A. (2004). "Designing Phase I $\overline{X}$ Charts with Small Sample Sizes". *Quality and Reliability Engineering International*, 20 (5): 497-510.

10. Gibbons, J.D., Chakraborti, S. (2010). Nonparametric Statistical Inference. 4th ed. Marcel Dekker, New York.

Appendix A: Detailed derivations

Appendix A provides detailed information and derivations relating to some of the equations presented in this paper.

1. Case KU

Results (A1) and (A2) are useful for deriving the conditional false alarm rate (*CFAR*) and the unconditional in-control average run-length (*ICARL*), for the $(\overline{X}, R)$ charting scheme and its component charts, in Case KU. Note that in Case KU, when the process is IC we have that

$$\overline{X}_i \sim N(\mu_0, \sigma^2/n) \quad \Rightarrow \quad Z_i = \frac{\sqrt{n}(\overline{X}_i - \mu_0)}{\sigma} \sim N(0,1) \qquad \text{(A1)}$$

Also,

$$\hat{\sigma} = \frac{\overline{R}}{d_2} \text{ is approximately distributed as } \frac{c\sigma\sqrt{U}}{\sqrt{v}} \qquad \text{(A2)}$$

where $U = \frac{v\hat{\sigma}^2}{c^2\sigma^2}$ follows a chi-square distribution with v degrees of freedom, the c and v depend on m and n (see Champ and Jones[9]). To calculate the constants c and v, we used the formulas given in Chen[3]. Note that c and v are not affected by the case (Case KU and Case UU) in hand, since $\hat{\sigma}$ is not dependent on μ.

Using (A1), (A2) and Equation (1), it can be shown that the *CFAR* and the unconditional *ICARL* of the $\overline{X}$ chart, with the estimated 3-sigma limits, in Case KU can be expressed as

$$
\begin{aligned}
& CFAR_{xbar}(U,m,n) \\
& = 1 - P\left(\left(\mu_0 - 3\frac{\hat{\sigma}}{\sqrt{n}} < \overline{X}_i < \mu_0 + 3\frac{\hat{\sigma}}{\sqrt{n}}\right) \mid IC\right) \\
& = 1 - P\left(\left(-3\frac{c\sqrt{U}}{\sqrt{v}} < Z_i < 3\frac{c\sqrt{U}}{\sqrt{v}}\right) \mid IC\right) \\
& = 1 - \Phi\left(3\frac{c\sqrt{U}}{\sqrt{v}}\right) + \Phi\left(-3\frac{c\sqrt{U}}{\sqrt{v}}\right)
\end{aligned}
\tag{A3}
$$

Since the conditional run-length distribution is geometric with success probability *CFAR* (Chakraborti[5]), the conditional *ICARL* equals $[CFAR_{xbar}(u,m,n)]^{-1}$. Hence the unconditional *ICARL* is given by

$$ICARL_{xbar}(m,n) = \int_0^\infty [CFAR_{xbar}(u,m,n)]^{-1} g(u)du \tag{A4}$$

where Φ is the cumulative distribution function (cdf) of the standard normal distribution.

It follows that the *CFAR* and the unconditional *ICARL* of the $\overline{X}$ chart, with the probability limits, in Case KU, can be expressed as

$$CFAR_{xbar}(U,m,n,p) = 1 - \Phi\left(z_{1-p/2}\frac{c\sqrt{U}}{\sqrt{v}}\right) + \Phi\left(-z_{1-p/2}\frac{c\sqrt{U}}{\sqrt{v}}\right) \tag{A5}$$

$$ICARL_{xbar}(m,n,p) = \int_0^\infty [CFAR_{xbar}(u,m,n,p)]^{-1} g(u)du \tag{A6}$$

respectively, where $z_{1-p/2}$ is the $(1-\frac{p}{2})^{th}$ percentile of the standard normal distribution.

Similarly, using (A2) and Equation (2), it can be shown that the *CFAR* and *ICARL* of the *R* chart, with the estimated 3-sigma limits, in Case KU, can be expressed as

$$\begin{aligned} &CFAR_R(U,m,n) \\ &= 1 - P\left(\left(D_3\overline{R} < R_i < D_4\overline{R}\right) \mid IC\right) \\ &= 1 - P\left(\left(D_3\frac{c\sqrt{U}}{\sqrt{v}} < W_i < D_4\frac{c\sqrt{U}}{\sqrt{v}}\right) \mid IC\right) \\ &= 1 - F_W\left(D_4\frac{c\sqrt{U}}{\sqrt{v}}\right) + F_W\left(D_3\frac{c\sqrt{U}}{\sqrt{v}}\right) \end{aligned} \tag{A7}$$

and

$$ICARL_R(m,n) = \int_0^\infty \left[CFAR_R(u,m,n)\right]^{-1} g(u)du \tag{A8}$$

respectively. Consequently, the *CFAR* and the unconditional *ICARL* of the *R* chart, with the probability limits, in Case KU, can be expressed as

$$\begin{aligned} &CFAR_R(U,m,n,p) \\ &= 1 - P\left(\left(F_W^{-1}\left(\frac{p}{2}\right)\hat{\sigma} < R_i < F_W^{-1}\left(1-\frac{p}{2}\right)\hat{\sigma}\right) \mid IC\right) \\ &= 1 - P\left(\left(F_W^{-1}\left(\frac{p}{2}\right)\frac{c\sqrt{U}}{\sqrt{v}} < W_i < F_W^{-1}\left(1-\frac{p}{2}\right)\frac{c\sqrt{U}}{\sqrt{v}}\right) \mid IC\right) \\ &= 1 - F_W\left(F_W^{-1}\left(1-\frac{p}{2}\right)\frac{c\sqrt{U}}{\sqrt{v}}\right) + F_W\left(F_W^{-1}\left(\frac{p}{2}\right)\frac{c\sqrt{U}}{\sqrt{v}}\right) \end{aligned} \tag{A9}$$

and

$$ICARL_R(m,n,p) = \int_0^\infty \left[CFAR_R(u,m,n,p)\right]^{-1} g(u)du \tag{A10}$$

respectively, where $F_W(w) = n\int_{-\infty}^{\infty}\left[\Phi(x+w) - \Phi(x)\right]^{n-1}\varphi(x)dx$ is the IC cdf of *W* (see for example, Gibbons and Chakraborti[10]) and F_W^{-1} is the inverse of the IC cdf of *W*.

Moreover, using (A3) and (A7) along with the independence between $\overline{X}_i$ and R_i in normal populations, it can be shown that the *CFAR* and the unconditional *ICARL* of the $(\overline{X}, R)$ charting scheme, with the estimated 3-sigma limits, in Case KU, can be written as

$$CFAR_{two-chart}(U,m,n) = 1-[1-CFAR_{xbar}(U,m,n)]\,[1-CFAR_R(U,m,n)] \tag{A11}$$

and

$$ICARL_{two-chart}(m,n) = \int_0^\infty [CFAR_{two-chart}(u,m,n)]^{-1} g(u)du \tag{A12}$$

respectively.

Similarly, using (A5) and (A9) with the independence assumption, the *CFAR* and the unconditional *ICARL* of the $(\overline{X}, R)$ charting scheme, with the probability limits, in Case KU, can be expressed as

$$CFAR_{two-chart}(U,m,n,p) = 1-[1-CFAR_{xbar}(U,m,n,p)]\,[1-CFAR_R(U,m,n,p)] \tag{A13}$$

and

$$ICARL_{two-chart}(m,n,p) = \int_0^\infty [CFAR_{two-chart}(u,m,n,p)]^{-1} g(u)du \tag{A14}$$

respectively.

2. Case UU

Note that, in Case UU, when the process is IC, the following is true

$$\overline{X}_i \sim N(\mu, \sigma^2/n) \;\Rightarrow\; Z_i = \frac{\sqrt{n}(\overline{X}_i - \mu)}{\sigma} \sim N(0,1) \tag{A15}$$

and

$$\hat{\mu} = \overline{\overline{X}} \sim N(\mu, \sigma^2/mn) \;\Rightarrow\; Z = \frac{\sqrt{mn}(\overline{\overline{X}} - \mu)}{\sigma} \sim N(0,1) \tag{A16}$$

Using (A15), (A16), (A2) and Equation (4), it can be shown that the *CFAR* and *ICARL* of the $\overline{X}$ chart, with the estimated 3-sigma limits, in Case UU, can be expressed as

$$
\begin{aligned}
&CFAR_{xbar}(U,m,n)\\
&=1-P\left(\left(\hat{\mu}-3\frac{\hat{\sigma}}{\sqrt{n}}<\overline{X}_i<\hat{\mu}+3\frac{\hat{\sigma}}{\sqrt{n}}\right)\mid IC\right)\\
&=1-P\left(\left(\frac{Z}{\sqrt{m}}-3\frac{c\sqrt{U}}{\sqrt{v}}<Z_i<\frac{Z}{\sqrt{m}}+3\frac{c\sqrt{U}}{\sqrt{v}}\right)\mid IC\right)\\
&=1-\Phi\left(\frac{Z}{\sqrt{m}}+3\frac{c\sqrt{U}}{\sqrt{v}}\right)+\Phi\left(\frac{Z}{\sqrt{m}}-3\frac{c\sqrt{U}}{\sqrt{v}}\right)
\end{aligned}
\tag{A17}
$$

and

$$ICARL_{xbar}(m,n)=\int_0^{\infty}\int_{-\infty}^{\infty}\left[CFAR_{xbar}(z,u,m,n)\right]^{-1}\phi(z)g(u)dzdu \tag{A18}$$

respectively, The constants *c* and *v* are calculated in the same way as in Case KU.

It then follows that the *CFAR* and *ICARL* of the $\overline{X}$ chart, with the estimated probability limits, in Case UU, can be expressed as

$$CFAR_{xbar}(Z,U,m,n,p)=1-\Phi\left(\frac{Z}{\sqrt{m}}+z_{1-p/2}\frac{c\sqrt{U}}{\sqrt{v}}\right)+\Phi\left(\frac{Z}{\sqrt{m}}-z_{1-p/2}\frac{c\sqrt{U}}{\sqrt{v}}\right) \tag{A19}$$

and

$$ICARL_{xbar}(m,n,p)=\int_0^{\infty}\int_{-\infty}^{\infty}\left[CFAR_{xbar}(z,u,m,n,p)\right]^{-1}\phi(z)g(u)dzdu \tag{A20}$$

respectively.

Moreover, using (A17) and (A7) along with the independence between $\overline{X}_i$ and R_i in normal populations, it can shown that the *CFAR* and the unconditional *ICARL* of the $(\overline{X},R)$ charting scheme, with the estimated 3-sigma limits, in Case UU can be written as

$$CFAR_{two-chart}(Z,U,m,n)=1-\left[1-CFAR_{xbar}(Z,U,m,n)\right]\left[1-CFAR_R(U,m,n)\right]. \tag{A21}$$

and

$$ICARL_{two-chart}(m,n)=\int_0^\infty\int_{-\infty}^\infty\left[CFAR_{two-chart}(z,u,m,n)\right]^{-1}\phi(z)g(u)dzdu \qquad \text{(A22)}$$

respectively.

Similarly, using (A19) and (A9) along with the independence assumption, the *CFAR* and the unconditional *ICARL* of the $(\overline{X},R)$ charting scheme, with the probability limits, in Case UU, can be expressed as

$$CFAR_{two-chart}(Z,U,m,n,p)=1-\left[1-CFAR_{xbar}(Z,U,m,n,p)\right]\left[1-CFAR_R(U,m,n,p)\right]. \qquad \text{(A23)}$$

and

$$ICARL_{two-chart}(m,n,p)=\int_0^\infty\int_{-\infty}^\infty\left[CFAR_{two-chart}(z,u,m,n,p)\right]^{-1}\phi(z)g(u)dzdu \qquad \text{(A24)}$$

respectively.

Appendix B: Software

Appendix B provides the R codes for the calculation of the unconditional *ICARL* of the $(\overline{X},R)$ charting scheme with the corrected limits in Case KU and Case UU, respectively.

B1. Unconditional *ICARL* for the $(\overline{X},R)$ charting scheme with corrected limits in Case KU

```
n=5 # sample size
m=c(5,30,100,500) # subgroup size
a=c(0.001288,0.001385,0.001371,0.001357) # charting constants
d2=function(n){
pt=function(w){1-ptukey(w,n,Inf)} # constant d2
integrate(pt,lower=0,upper=Inf)[[1]]}
d2=d2(n)
EW2=function(n){
ptt=function(a){(1-ptukey(sqrt(a),n,Inf))}
integrate(ptt,lower=0,upper=Inf)[[1]]}
d3=function(n){
sqrt(EW2(n)-d2^2)} # constant d3
d3=d3(n)

library(cubature)
```

```
ICARL=function(m,aa){
M=function(m){
d3^2/(m*d2^2)}
r=function(m){
(-2+2*sqrt(1+2*M(m)))^-1}
t=function(m){
M(m)+1/(16*r(m)^3)}
v=function(m){
(-2+2*sqrt(1+2*t(m)))^-1} # degrees of freedom v
cc=function(m){
1+(1/(4*v(m)))+(1/(32*v(m)^2))-(5/(128*v(m)^3))} # constant c
uclxbar=function(x){qnorm(1-a[j]/2,0,1)*cc(m)*sqrt(x)/sqrt(v(m))} # ucl xbar chart
lclxbar=function(x){-qnorm(1-a[j]/2,0,1)*cc(m)*sqrt(x)/sqrt(v(m))} # lcl xbar chart
PNSxbar=function(x){pnorm(uclxbar(x),0,1)-pnorm(lclxbar(x),0,1)}# Probability of
no signal for the xbar chart
uclrchart=function(x){qtukey(1-a[j]/2,n,Inf)*cc(m)*sqrt(x)/sqrt(v(m))}# ucl R chart
lclrchart=function(x){qtukey(a[j]/2,n,Inf)*cc(m)*sqrt(x)/sqrt(v(m))} # lcl R chart
PNSrchart=function(x){ptukey(uclrchart(x),n,Inf)-
ptukey(max(c(lclrchart(x),0)),n,Inf)} # Probability of no signal for the R chart
CFAR=function(x){1-PNSxbar(x)*PNSrchart(x)} # Conditional Probability of a
signal for the corrected limits (Xbar,R) charting scheme
CARL=function(x){ CFAR(x)^-1*dchisq(x,v(m))} # Conditional ICARL for the
corrected limits (Xbar,R) charting scheme
b=qchisq(0.99999,v(m))
adaptIntegrate(CFAR,c(0),c(b),tol=1e-10)[[1]]} # Marginal ICARL for the
corrected limits (Xbar,R) charting scheme

ICARLxbarrchart=numeric(length(a))
for (j in 1:length(m)) {
ICARLxbarrchart[j]= ICARL(m[j],a[j])}
ICARLxbarrchart ]]} # Marginal ICARL for the corrected limits (Xbar,R)
charting scheme
```

B2. Unconditional *ICARL* of the $(\overline{X}, R)$ charting scheme with corrected limits in Case UU

```
n=5 # sample size
m=c(5,30,100,500) # subgroup sizes
a=c(0.001025,0.001290,0.001337,0.001350) # charting constants
d2=function(n){
pt=function(w){1-ptukey(w,n,Inf)}
integrate(pt,lower=0,upper=Inf)[[1]]} # constant d2
d2=d2(n)
EW2=function(n){
ptt=function(a){(1-ptukey(sqrt(a),n,Inf))}
integrate(ptt,lower=0,upper=Inf)[[1]]}
d3=function(n){
sqrt(EW2(n)-d2^2)} # constant d3
d3=d3(n)
```

```
library(cubature)
ICARL=function(m,a){
M=function(m){
d3^2/(m*d2^2)}
r=function(m){
(-2+2*sqrt(1+2*M(m)))^-1}
t=function(m){
M(m)+1/(16*r(m)^3)}
v=function(m){
(-2+2*sqrt(1+2*t(m)))^-1} # degrees of freedom v
cc=function(m){
1+(1/(4*v(m)))+(1/(32*v(m)^2))-(5/(128*v(m)^3))} # constant c
uclxbar=function(x){x[1]/sqrt(m)+qnorm(1-a[j]/2,0,1)*cc(m)*sqrt(x[2])/sqrt(v(m))} # ucl xbar chart
lclxbar=function(x){x[1]/sqrt(m)-qnorm(1-a[j]/2,0,1)*cc(m)*sqrt(x[2])/sqrt(v(m))} # ucl xbar chart
PNSxbar=function(x){pnorm(uclxbar(x),0,1)-pnorm(lclxbar(x),0,1)} # Probability of no signal for the xbar chart
uclrchart=function(x){ qtukey(1-a[j]/2,n,Inf) *cc(m)*sqrt(x[2])/sqrt(v(m))}# ucl R chart
lclrchart=function(x){ qtukey(a[j]/2,n,Inf) *cc(m)*sqrt(x[2])/sqrt(v(m))} # lcl R chart
PNSrchart=function(x){ptukey(uclrchart(x),n,Inf)-
ptukey(max(c(lclrchart(x),0)),n,Inf)} # Probability of no signal for the R chart
AFAR=function(x){1-PNSxbar(x)*PNSrchart(x)}
CICARL=function(x){ AFAR(x)^-1*dnorm(x[1],0,1)*dchisq(x[2],v(m))} # Conditional ICARL for the corrected limits (Xbar,R) charting scheme
b=qchisq(0.99999,v(m))
adaptIntegrate(CICARL,c(-100,0),c(100,b),tol=1e-10)} # Marginal ICARL for the corrected limits (Xbar,R) charting scheme

ICARLxbarrchart=numeric(length(m))
for (j in 1:length(m)) {
ICARLxbarrchart[j]= ICARL(m[j],a[j])[[1]]}
ICARLxbarrchart # Marginal ICARL for the corrected limits (Xbar,R) charting scheme
```